# Paramagnetic and Diamagnetic Cerebral Lesions in Susceptibility Weighted Phase Imaging (SWI)

**A. Deistung[1], A. Rauscher[1], H-J. Mentzel[2], S. Witoszynskyj[1], W. A. Kaiser[3], and J. R. Reichenbach[1]**

[1]Medical Physics Group, Institute of Diagnostic and Interventional Radiology, Friedrich Schiller-University, Jena, Germany, [2]Department of Pediatric Radiology, Institute of Diagnostic and Interventional Radiology, Friedrich Schiller-University, Jena, Germany, [3]Institute of Diagnostic and Interventional Radiology, Friedrich Schiller-University, Jena, Germany

## Introduction

One essential problem in medical diagnostics of cerebral malformations is among other things the discrimination between calcifications and (micro-)hemorrhages, which is often not unequivocally possible with conventional $T_1$-, $T_2$-, $T_2^*$- or FLAIR-weighted images. One possible criterion for the discrimination of such lesions may be the magnetic susceptibility. In recent years, the method of susceptibility weighted imaging (SWI) has proven its potential for the detection of blood products and tissue with different magnetic susceptibility [1]. The phase from SWI data corresponds to local changes in the magnetic field and is thus sensitive to susceptibility changes caused by small lesions. In this study we explore the feasibility to characterize nearly spherical perturbers with susceptibility weighted phase imaging to differentiate between paramagnetic and diamagnetic lesions.

## Theory and Methods

A spherical object with a magnetic susceptibility different than the surrounding tissue leads to modifications in the z-component $\Delta B_z$ of the static magnetic field $B_0$ and is given inside the sphere by [2]:

$$\Delta B_z = \frac{2 \cdot \Delta\chi \cdot B_0}{3} \qquad r < a \qquad (1)$$

and outside the sphere by:

$$\Delta B_z(r,\phi) = \frac{\Delta\chi \cdot B_0}{3} \cdot \left(\frac{a}{r}\right)^3 \cdot \left(3 \cdot \cos^2\phi - 1\right) \qquad r > a, \qquad (2)$$

where r and $\phi$ are the polar coordinates, $\Delta\chi$ is the difference in magnetic susceptibility between the sphere and its surroundings $\Delta\chi = \chi_{int} - \chi_{ext}$, and $a$ is the radius of the sphere. The shape of this field distortion is schematically displayed in Figure 1. For positive $\Delta\chi$ the field strength is increased above and below the discontinuity and reduced near the equatorial plane of the dipole. For perturbers with a negative $\Delta\chi$ the effect is inversed. Since the phase of the SWI sequence is sensitive to changes in the local magnetic field, it can be used to determine whether an approximately spherical lesion is more paramagnetic or more diamagnetic than the surrounding tissue. Patient data were acquired on a 1.5T MR-System (Magnetom Vision, Siemens Medical Solutions, Erlangen, Germany) in axial orientation with the standard CP transmit/receive head coil using a 3D velocity compensated gradient-echo sequence (TE/TR/$\alpha$ = 40 ms / 67 ms / 25 °, typical FoV = 256 x 192 x 72 mm$^3$, typical matrix = 512 x 256 x 36). Unwanted phase jumps were removed by phase unwrapping [3, 4]; however, it can be incomplete and limited within the area of the lesion (blue box on the right in Figure 2 (c))

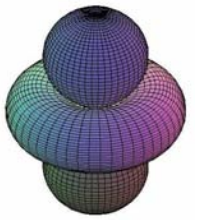

***Figure 1:*** *Iso-surface of the perturbation of $\Delta B_z$ induced by a spherical discontinuity in $\Delta\chi$. This spherical source is located at the centre of the torus between the two lobes. For a given susceptibility difference, $\Delta\chi$, the torus and both lobes have opposite sign.*

## Results

Cavernous malformations are characterized by spherical sinusoidal vascular spaces containing clotted or unclotted blood in various stages of oxidation producing field distributions that are typical for paramagnetic lesions (Fig. 2(a)). In magnitude and phase images cavernomas with diameters down to 1-2 mm could be detected (Fig. 2(b)). For another patient the differential diagnosis of an old hemorrhage or a calcified tumor was resolved due to the diamagnetic dipole structure in the phase (Fig. 2(c)) which leads to the final diagnosis of a calcified tumor. Figure 2(d) displays the SWI phase image of a patient with tuberous sclerosis whose subependymal nodules are calcified (which is among other things one typical pattern for this disease).

## Discussion

The field distribution not only helps to differentiate between different types of lesions, they also act as a loupe, so that lesions with sub-voxel diameters can be detected. The method was only demonstrated on axial images, where higher and lower slices correspond to above and below the lesion. The classification of lesions also works for coronal and sagittal acquisition and the assessment of such images is straight forward. When using phase information, one has to keep in mind that the effects produced by a lesion not only depend on its magnetic susceptibility but also on its own shape and the shape of the tissue in which it is embedded. Moreover, the visualization of the phase is also scanner specific. On some MR scanners bright areas in phase images correspond to a decreased resonance frequency (as in all cases shown herein), and on other MR systems to an increased resonance frequency. In contrast to brain tissue oxyhemoglobin, methomoglobin, hemosiderin, and ferritin are more paramagnetic, whereas bone minerals, dystrophic calcification, and tumoral calcification commonly possess more diamagnetic susceptibilities [5]. In summary, investigation of the phase information obtained with SWI, which comes at no additional acquisition time, may not only be helpful to better classify certain cerebral lesions but may also facilitate the final diagnosis.

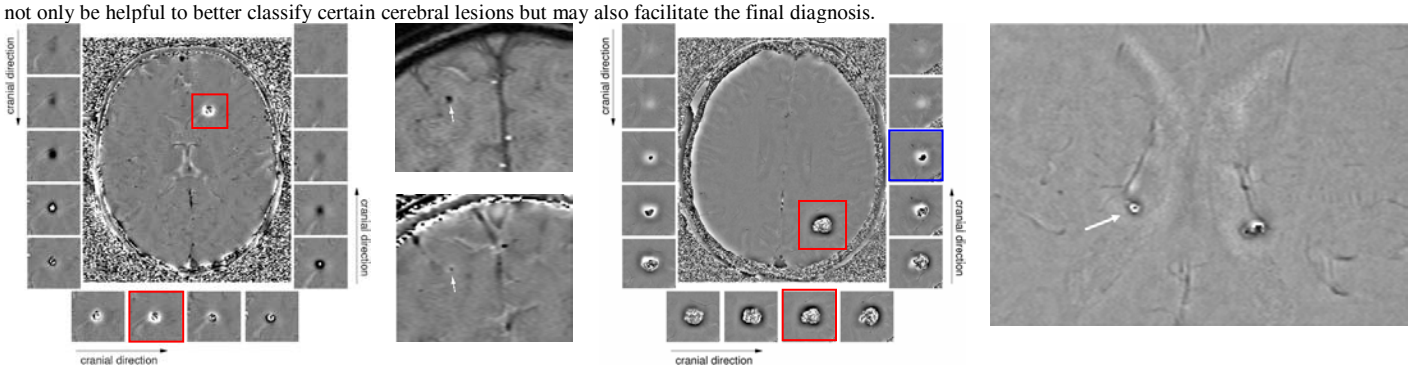


***Figure 2:*** *(a) A 12-month girl with multiple cavernous lesions. The large image shows the phase in the equatorial plane of the dipole. In the small bordering phase images the typical pattern of the paramagnetic dipole is sampled from caudal (top left) to cranial (top right) with 1.5 mm thick slices. These images clearly demonstrate that the phase is reduced below and above the equatorial plane, in which the lesion itself is depicted by a dark spot surrounded by a bright rim. (b) Small cavernomas (arrow) are visualized in the axial SWI magnitude image (top). The paramagnetic nature of the lesion was classified in the corresponding phase image (bottom) due to the typical bright equatorial rim. (c) The phase images of this 42-years old patient illustrate a diamagnetic lesion sampled with 1 mm slice thickness. The final diagnosis was a calcified tumor. The diamagnetic dipole is characterized by a dark equatorial rim with bright lobes. (d) A patient with tuberous sclerosis. The SWI phase image demonstrates a calcification of the subependymal nodules with a bright spot and hypointense rim (arrow) which corresponds to a diamagnetic lesion.*

## References

[1] Reichenbach JR et al. Radiology. 1997; 204(1): 272-277
[2] Schenck JF, Med. Phys. 1996; 23(6): 815-850
[3] Witoszynskyj S et al, Proc. of the ISMRM. 2005: 439
[4] Rauscher A et al. J Magn Reson Imag. 2003, 18(2): 175-180
[5] Anderson HC, Pathol Annu 1980; 15:45-75